

1 **Supporting information for**

2 **Effect of steam on heat storage and attrition performance of limestone**
3 **under fluidization during CaO/CaCO₃ heat storage cycles**

4 Yi Fang^a, Yingjie Li^{a,*}, Yehui Dou^a, Zirui He^b, Jianli Zhao^a

5 ^a Shandong Engineering Laboratory for High-efficiency Energy Conservation and Energy Storage
6 Technology & Equipment, School of Energy and Power Engineering, Shandong University, Jinan 250061, China

7 ^b Institute of Mechanics, Materials and Civil Engineering (iMMC), Materials & Process Engineering
8 (IMAP), Université Catholique de Louvain, Place Sainte Barbe 2, B-1348 Louvain-la-Neuve, Belgium

9
10
11
12
13
14
15
16

* Corresponding author: E-mail: liyj@sdu.edu.cn (Y. Li).

17 The numerical model

18 In this work, the CFD-DEM model was used to simulate hydrodynamics, heat transfer, and the heterogeneous
19 reaction of CaO/CaCO₃ heat storage. The mass and momentum conservation equations are shown as follows:

$$20 \quad \frac{\partial \rho}{\partial t} + \nabla \cdot (\rho \mathbf{v}) = s_1 \quad (S1)$$

$$21 \quad s_1 = MWw \quad (S2)$$

$$22 \quad \frac{\partial}{\partial t} (\rho \cdot \mathbf{v}) + \nabla \cdot (\rho \cdot \mathbf{v} \cdot \mathbf{v}) = -\nabla p + \nabla \cdot \bar{\bar{\tau}} + \rho \mathbf{g} + \mathbf{F} \quad (S3)$$

23 where ρ is density, kg·m⁻³; \mathbf{v} is velocity, m·s⁻¹; p is static pressure, Pa; τ is stress tensor, N·m⁻²; s_1 is the mass source
24 term for the specie, kg·m⁻³s⁻¹; MW is molecular weight, kg mol⁻¹; w is molar production rate, mol·m⁻³s⁻¹; \mathbf{F}
25 **Error!Error!** is the force applied by particles, N.

26 The force equation of a single particle is as follows:

$$27 \quad m_p \frac{d\mathbf{u}_p}{dt} = \mathbf{F}_{\text{drag}} + \mathbf{F}_{\text{pressure}} + \mathbf{F}_{\text{gravity}} + \sum_1^N (\mathbf{F}_N + \mathbf{F}_T) \quad (S4)$$

28 where m_p is particle mass, kg; \mathbf{u}_p is particle velocity, m·s⁻¹; \mathbf{F}_{drag} is the drag force given by Gidaspow, N; $\mathbf{F}_{\text{pressure}}$
29 is the force of pressure, N; $\mathbf{F}_{\text{gravity}}$ is the force of gravity, N; \mathbf{F}_N and \mathbf{F}_T represent normal and tangential components
30 of the contact force.

31 To simplify the calculation, radiation heat transfer was ignored, energy conservation equations for particles
32 and continuous phases are shown as follows:

$$33 \quad m_p c_p \frac{dT_p}{dt} = hA_p (T_\infty - T_p) - \frac{dm_p}{dt} \Delta H \quad (S5)$$

$$34 \quad \frac{\partial}{\partial t} (\rho E) + \nabla \cdot (\mathbf{v}(\rho E + p)) = \nabla \cdot \lambda \nabla T + S_h + S_q \quad (S6)$$

35 where c_p is the specific heat capacity of the particles, J·g·K⁻¹; T_p is the temperature of the particles, K; h is the heat
36 transfer coefficient, W·m⁻²·K⁻¹; E is the internal energy, J; λ is the effective conductivity, W·m⁻¹·K⁻¹; S_q is the heat
37 source due to gas-particle convective heat transfer, J·mol⁻¹; S_h is the heat from the interphase transferred mass, J.

38 In this reaction, the heat of the reaction ΔH is released from the particles.

39 Species transport equation of gas species i is shown as follows:

$$40 \quad \frac{\partial}{\partial t}(\rho Y_i) + \nabla \cdot (\rho \mathbf{v} Y_i) = -\nabla \cdot \mathbf{j}_i + R_i \quad (S7)$$

41 where Y_i is the mass fraction of the gas; \mathbf{j}_i is diffusion coefficient of gas, $\text{kg} \cdot \text{m}^{-2} \cdot \text{s}^{-1}$; R_i is production rate of species
42 due to the heterogeneous reaction m^{-3} .

43 The heterogeneous reaction of CO_2 and CaO is a complex process. To simplify the model, it is assumed that
44 the particle size is constant during the reaction. The apparent reaction rate was determined by Sun ¹:

$$45 \quad R = \frac{dX}{dt(1-X)} 56k(P_{\text{CO}_2} - P_{\text{eq}})^n S \quad (S8)$$

46 Where R is apparent reaction rate, s^{-1} ; X is the conversion of CaO ; P_{CO_2} is the partial pressure of CO_2 , KPa ; P_{eq} is
47 the equilibrium partial pressure of CO_2 , KPa . S is the specific surface area of the CaO , m^2/g . The value of k and n
48 is determined by the difference between the CO_2 partial pressure and the equilibrium partial pressure:

$$49 \quad k = 1.67 \times 10^{-3} \exp\left(\frac{-29}{0.008314T_p}\right), n = 0, (P_{\text{CO}_2} - P_{\text{eq}}) > 10; \quad (S9)$$

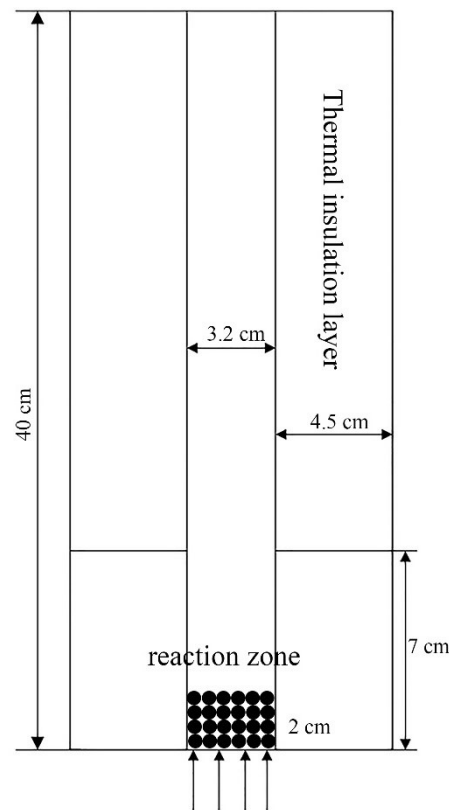
$$50 \quad k = 1.67 \times 10^{-4} \exp\left(\frac{-29}{0.008314T_p}\right), n = 1, (P_{\text{CO}_2} - P_{\text{eq}}) < 10; \quad (S10)$$

51 Reactor geometry

52 The reactor was simplified as a 12.6×40 pseudo-3D fluidized bed as shown in Fig. S1. The diameter of the
53 furnace was 3.2 cm, the width of the insulation layer was 4.5 cm, and the limestone particles with a height of 2 cm
54 were placed at the bottom of the furnace. The gas entered from the bottom and the outlet was the pressure-outlet.
55 Before the reaction, the wall surface of the reaction zone was set as a constant temperature at $600 \text{ }^\circ\text{C}$ and particles
56 were fluidized for 10 s. After the simulation was stable, the chemical reaction module was turned on and the wall
57 surface of the reaction zone was changed to fluid-solid temperature coupling. Table 1 lists the parameters of the
58 simulated system.

59 Table S1 Computational parameter.

Bed size, cm × cm	12.6×40	Fluid time step, s	1×10 ⁻⁵
CFD cells number	63×200×1	DEM time step, s	4×10 ⁻⁶
Particles number	10850	Particle normal stiffness, N/m	1000
Particle diameter, m	0.0002	Particle normal restitution coeff.	0.9
Inlet gas velocity, m/s	0.052	Particle frictional coefficient	0.1
Inlet gas temperature, °C	30 °C	Particle tangential stiffness, N/m	285
Inlet gas temperature, °C	27 °C	Particle tangential restitution coeff.	0.3
Initial particle temperature, °C	600 °C		



60

61

Fig. S1. Computational domain of the bubbling fluidized bed reactor.

62 Model validation

63 Fig. S2 presents the simulation results of bed pressure drop and bed temperature during exothermic stage.

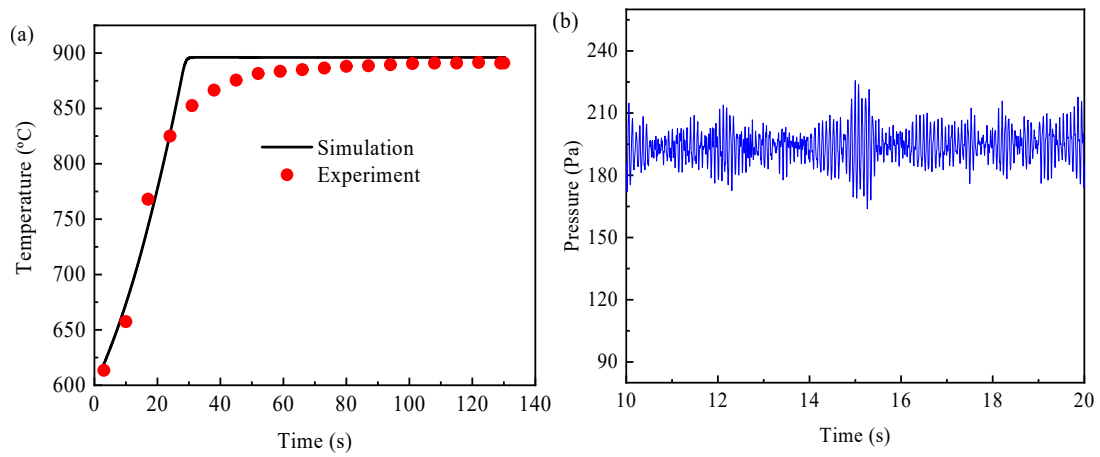
64 The bed pressure drop reflects the fluidization state of particles. In 10-20s, the simulated pressure drop is shown

65 in Fig. S2(b). The average pressure drop in our calculation results is 192 Pa, and the predicted value calculated

66 according to the Ecuadorian formula² is 188 Pa, which is about 97% of our simulated value. It is generally believed

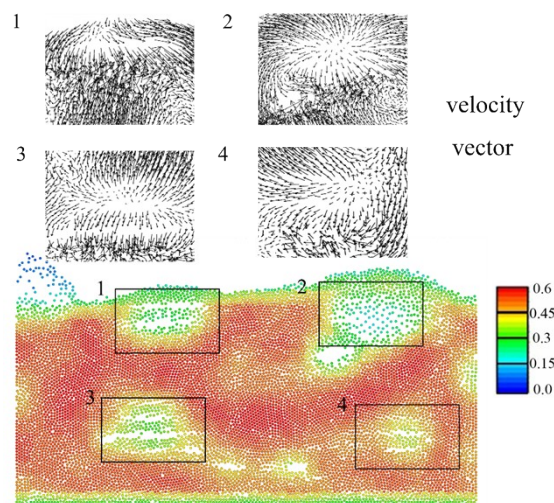
67 that the error is within 10% to be reliable³. The change of bed temperature reflects the chemical reaction and heat

68 transfer between gas and solid. The simulated temperature curve in Fig. S2(a) fits well with the measured
69 temperature curve except in the temperature transition region. This is because the reaction kinetics formula used
70 in the simulation does not represent the transition region well, but it has a negligible effect on the simulation
71 results. The comparison in the simulation and experimental results shows that the CFD-DEM model is reasonable
72 for calculating the exothermic process of calcined limestone.



73

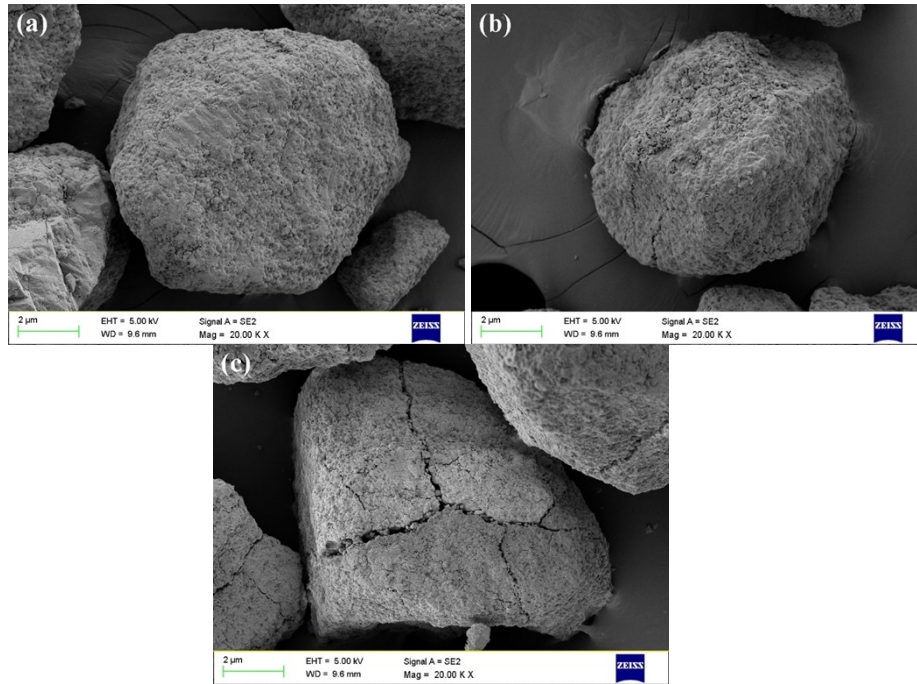
74 Fig. S2. Comparison in simulation and experimental results: (a) bed temperature, (b) bed pressure drop.



75

76

Fig. S3. Snapshots of particle dynamics (particles colored by volume fraction).



77

78

79 Fig. S4. SEM images of the original calcined limestone and the calcined limestone under different calcination and
80 carbonation atmospheres: (a) original calcined limestone, 700×; (b) limestone 80% H₂O/20% CO₂ mixture and
81 carbonated under 20% H₂O/80% CO₂ mixture after 10 cycles, 20000×; (c) limestone calcined under steam and
82 carbonated under CO₂ after 10 cycles, 20000×.

83 References

- 84 1. P. Sun, J. R. Grace, C. J. Lim and E. J. Anthony, *Chemical Engineering Science*, 2008, **63**, 47-56.
- 85 2. S. Ergun, *Journal of Materials Science and Chemical Engineering*, 1952, **48**, 89-94.
- 86 3. Y. Zhang, M. Ye, Y. Zhao, T. Gu, R. Xiao and Z. Liu, *Powder Technology*, 2015, **275**, 199-210.

87